# Thermal stability and crystallochemical analysis for $Co^{II}$-based coordination polymers with TPP and TPPS porphyrins

**Arkaitz Fidalgo-Marijuan,[a] Gotzone Barandika,*[b] Begoña Bazán,[a] Miren-Karmele Urtiaga[a] and María Isabel Arriortua[a]**

***Received (in XXX, XXX) Xth XXXXXXXXX 20XX, Accepted Xth XXXXXXXXX 20XX***
**DOI: 10.1039/b000000x**

Two new CoP-bipy compounds have been synthesised and characterised, where P is TPP for compound **1** (TPP= *meso*-tetraphenylporphyrin) and TPPS for compound **2** (TPPS= *meso*-tetraphenylporphine-tetrasulfonic acid tetrasodium salt), and bipy is 4,4´-bipyridine. Compound **1** consists of 1D polymers packed in a network where isolated porphyrin units are immobilized by an extended π-bond system. On the other hand, as we are aware, compound **2** is the first Co-TPPS compound in literature. It also consists of 1D polymers that are formed by the alternation of two distinct metal centres. These unprecedented polymers are packed forming cavities where crystallization molecules of water are located. The robustness of the hydrogen bond system and a topology based on interpenetrated nets are responsible for the high thermal stability of compound **2**. Additionally, a crystallochemical study confirmed the existence of a correlation between the degree of ruffled distortion of the porphyrin macrocycle and some selected dihedral angles and distances for $Co^{II}$ porphyrins in literature.

## Introduction

Metal-organic frameworks (MOFs) have emerged as an interesting class of porous solids that can be constructed from a variety of molecular complexes[1-4] and explored for a range of applications in gas storage,[5,6] compound separation,[7,8] chemical sensing,[9-12] nonlinear optics,[13] biomedical imaging,[14-16] drug delivery,[17-19] and heterogeneous catalysis.[20-23] On the other hand, it is worth mentioning that facile chemical modification, high thermal and chemical stability allow metalloporphyrins to be remarkable catalysts for numerous reactions.[24-26] In particular, porous metalloporphyrinic frameworks have great potential to act as heterogeneous catalysts with shape- and size-selectivity. In this sense, Suslick *et al*. must be cited as they first demonstrated the catalytic property of a porphyrinic MOF.[27]

In this context, metalloporphyrins are remarkable precursors in supramolecular chemistry, giving rise to a variety of materials because of their unique chemical, physical and biological properties.[28-30] In order to enhance the connectivity between metal centres, a secondary ligand can be used in porphyrinic systems. In fact, the Choe group demonstrated that a range of metalloporphyrinic frameworks can be generated by using porphyrin metallo-ligands and bipyridyl molecules.[31] However, it must be pointed out that research on the applications of porphyrinic MOFs is just in the initial stage.[32]

Taking into account the above mentioned aspects, this work was focused on the preparation of metalloporphyrin-based coordination networks. Our strategy also includes the use of different bipyridyl ligands, as they have been observed to produce a variety of porphyrin-based MOFs.[33] In addition, we have a large experience with these connectors.[34-39] In this context, we have been exploring CoP-bipy combinations where P is either TPP (TPP=*meso*-tetraphenylporphyrin) or TPPS (TPPS= *meso*-tetraphenylporphine-tetrasulfonic acid tetrasodium salt), and bipy is 4,4´-bipyridine. It is worth mentioning that just four crystalline compounds have been reported for TPPS-based metalloporphyrins,[40-42] and none of them has cobalt. On the other hand, even if the number of TPP-based metalloporphyrins is higher, the number of Co-based compounds exhibiting extended networks is also significantly low.[43,44]

Thus, the work herein presented consists of the synthesis and characterisation of two new CoP-bipy compounds where the metal ion is $Co^{II}$ and P is TPP for compound **1**, and TPPS for compound **2**. Both of them have been structurally characterised by single-crystal X-ray diffraction (XRD) and IR and EPR spectroscopies. Thermal stability has been explored by means of thermogravimetry (TGA), and X-ray thermodiffractometry (TDX).

Distortion of macrocycles is biologically relevant[45] and influences physical[46,47] and chemical[48,49] properties of porphyrin complexes. In this sense, we have also analysed the out-of-plane displacement of porphyrin backbones for both compounds. In order to contextualise this analysis the study was extended to all the $Co^{II}$ porphyrins found in the CSD. A similar study has been previously reported for $Co^{III}$ porphyrins.[50]

## Experimental section

### General

All solvents and chemicals were used as received from reliable commercial sources. The reagents *meso*-tetraphenyl-porphine cobalt (II) (CoTPP), *meso*-tetraphenyl porphine-4,4′,4″,4‴-tetrasulfonic acid tetrasodium salt (TPPS), Cobalt (II) nitrate hexahydrate 99% and 4,4'-bipyridine 98% (bipy) and the solvent *N*,*N*-dimethylformamide (DMF) 99.8% were purchased from Sigma-Aldrich Co.; ethanol absolute was purchased from Panreac.

### Synthesis of compounds 1 and 2

**$[CoTPP(bipy)]\cdot([CoTPP])_{0.22}\cdot(TPP)_{0.78}$ (1).** *meso*-tetraphenyl-porphine cobalt (II) (6.7 mg, 0.01 mmol), 4,4´-bipyridine (9.4 mg, 0.06 mmol) and 40 μL NaOH (3M) were added to a mixture of DMF (3 mL) and ethanol (1 mL) in a small capped vial, sonicated to ensure homogeneity and heated to 120 ºC for 48 h, following by slow cooling to room temperature at 2 ºC/h, yielding diffraction quality prismatic dark blue crystals. (Found: C, 79.5(3); H, 4.60(4); N, 10.00(2). Calc. for $C_{98}H_{65.56}Co_{1.22}N_{10}$: C, 80.89; H, 4.54; N, 9.62). $\nu_{max}/cm^{-1}$ 3052 and 3028 ($C(sp^2)H$), 1596-1441 (CC), 1349 (CN), 1210 and 1069 (bipy), 1000 (CoTPP) and 795-700 (CH) (Fig. S1, ESI†).

**$[CoTPPS_{0.5}(bipy)(H_2O)_2]\cdot 6H_2O$ (2).** *meso*-tetraphenyl porphine-4,4′,4″,4‴-tetrasulfonic acid tetrasodium salt (10.2 mg, 0.01 mmol) and $Co(NO_3)\cdot 6H_2O$ (5.8 mg, 0.02 mmol) were dissolved in distilled water (10 mL) and the solution was stirred for 30 min. Then, 4,4´-bipyridine (9.4 mg, 0.06 mmol) was dissolved in hot (70 ºC) distilled water (5 mL) and added to the mixture in a 100 mL CEM EasyPrep microwave vessel. The mixture was heated by microwave under autogenous pressure at 160 ºC for 2 h, and then cooled naturally to room temperature, yielding diffraction quality prismatic dark blue crystals. (Found: C, 45.8(3); H, 4.47(3); N, 6.89(2); S, 7.80(3). Calc. for $C_{32}H_{36}CoN_4O_{14}S_2$: C, 46.66; H, 4.40; N, 6.80; S, 7.79). $\nu_{max}/cm^{-1}$ 3397 (OH), 1624-1410 (CC), 1394 and 1174 (SO), 1349 (CN), 1208 and 1076 (bipy), 1000 (CoTPPS) and 863-744 (CH) (Fig. S2, ESI†).

### Single-crystal X-ray diffraction

Prismatic dark blue single-crystals of compounds **1** and **2** with dimensions given in Table 1 were selected under polarizing microscope and mounted on MicroMounts. Single-crystal X-ray diffraction data were collected at 100 K on a SuperNova single source diffractometer with Cu-Kα radiation (λ=1.5418 Å). The Lorentz-polarization and absorption corrections were made with the diffractometer software, taking into account the size and shape of the crystals.[51]

The structure of compound **1** was solved in the monoclinic *C*2/*c* space group with SIR-92[52] program, which allowed us to obtain the position of Co atoms, as well as nitrogen and some of the carbon atoms of the TPP and bipyridine molecules. The refinement of the crystal structure was performed by full matrix least-squares based on $F^2$, using the SHELXL-97 program[53] obtaining the remaining carbon atoms. Anisotropic thermal parameters were used for all non-hydrogen atoms (Fig. S3, ESI†). All the hydrogen atoms, connected to the aromatic rings (C-H 0.95Å) were fixed geometrically and were refined using a riding model with common isotropic displacements.

Compound **2** was solved in the tetragonal $I\,4_1/a$ space group with Superflip[54] program, which allowed us to obtain the position of Co atoms, as well as nitrogen and some of the carbon atoms of the TPPS and bipyridine molecules. The refinement of the crystal structure was performed by full matrix least-squares based on $F^2$, using the SHELXL-97 program[53] obtaining the remaining carbon atoms and the oxygen and sulphur atoms of the porphyrin and water molecules. Anisotropic thermal parameters were used for all non-hydrogen atoms (Fig. S4, ESI†). All the hydrogen atoms, connected to the aromatic rings (C-H 0.95 Å) were fixed geometrically and were refined using a riding model with common isotropic displacements. The position of the hydrogen atoms bonded to the coordination water molecule were fixed using DFIX and DANG instructions in the refinement to adjust the O-H distance to 0.82 Å and the H-O-H angle to 112º, respectively. All of the crystallization molecules of water for compound **2** were disordered in two groups of three water molecules. The hydrogen atoms of these water molecules were not considered due to the lack of density in the residual density map. Crystal data for both structures are listed in Table 1. Atomic coordinates, anisotropic thermal parameters and hydrogen atom coordinates for both compounds are given in Tables S1, S2, S3, S4, S5 and S6, ESI†.

**Table 1** Details of the crystal data, structural resolution and refinement procedure for **1** and **2**.

| | **1** | **2** |
|---|---|---|
| Formula | $C_{98}H_{65.56}Co_{1.22}N_{10}$ | $C_{32}H_{36}CoN_4O_{14}S_2$ |
| FW, g·mol$^{-1}$ | 1455.06 | 811.62 |
| *a*, Å | 25.1252(4) | 17.9776(2) |
| *b*, Å | 11.7811(2) | |
| *c*, Å | 23.9790(4) | 22.3567(3) |
| *β*, deg | 93.5960(10) | |
| *V*, Å$^3$ | 7083.9(2) | 7225.55(15) |
| Space group | *C*2/*c* | $I\,4_1/a$ |
| *Z* | 4 | 8 |
| $\rho_{obs}$, $\rho_{cal}$, g·cm$^{-3}$ | 1.371(6), 1.364 | 1.488(4), 1.492 |
| *F*(000) | 3026 | 3320 |
| *μ*, mm$^{-1}$ | 2.761 | 5.445 |
| Crystal size, mm | 0.26 x 0.19 x 0.06 | 0.12 x 0.12 x 0.021 |
| Absorption correction | Multi-scan | Analytical |
| Radiation, λ, Å | 1.54184 | 1.54184 |
| Temperature, K | 100(2) | 100(2) |
| Reflections collected, unique | 25120, 7352 ($R_{int}$ = 0.0405) | 23662, 3774 ($R_{int}$ = 0.096) |
| Limiting indices | -29<=*h*<=31<br>-14<=*k*<=14<br>-30<=*l*<=23 | -22<=*h*<=22<br>-14<=*k*<=22<br>-28<=*l*<=25 |
| Refinement method | Full-matrix least-squares on $F^2$ | Full-matrix least-squares on $F^2$ |
| R1, wR2 [I > 2σ(I)] | R1 = 0.0416, wR2 = 0.1095 | R1 = 0.0669, wR2 = 0.1845 |
| R1, wR2 (all data) | R1 = 0.0438, wR2 = 0.1115 | R1 = 0.0856, wR2 = 0.2040 |
| Goodness of fit on $F^2$ | 1.056 | 1.051 |
| Parameters /restraints | 504 / 0 | 274 / 3 |

### Physicochemical characterisation techniques

The IR spectra were collected on a JASCO FT/IR-6100 spectrometer at room temperature at the range of 4000-400 cm$^{-1}$, in KBr pellets (1% of the sample). C, H, N and S elemental analyses were measured using a Euro EA 3000 elemental

analyser. Electron paramagnetic resonance (EPR) spectra were measured with a Bruker ESP-300 spectrometer operating at X band and equipped with a nitrogen and helium cryostat.

The thermal analyses were carried out in air atmosphere using a NETZSCH STA 449F3 instrument for compound **1** and SDT 2960 Simultaneous DSC-TGA TA Instruments for **2**. A crucible containing approximately 10 mg of sample was heated at 5 ºC $min^{-1}$ in the temperature range 30-600 ºC. The thermal behaviour was also studied using X-ray thermodiffractometry. A Bruker D8 Advance Vantec diffractometer (Cu-Ka radiation) equipped with a variable-temperature stage (Anton Paar HTK2000) with a Pt sample holder was used in the experiments. The powder patterns were recorded in $2\theta$ steps of 0.0333º in the 5-38º range, counting for 0.8 s per step and increasing the temperature at 10 ºC·$min^{-1}$ from room temperature to 550 ºC.

## Results and discussion

### Crystal structures

The crystal structure for compound **1** consists of 1D polymers extending along the [010] direction where CoTPP units are axially bonded to two bipy ligands resulting in a porous coordination network (Fig. 1a).

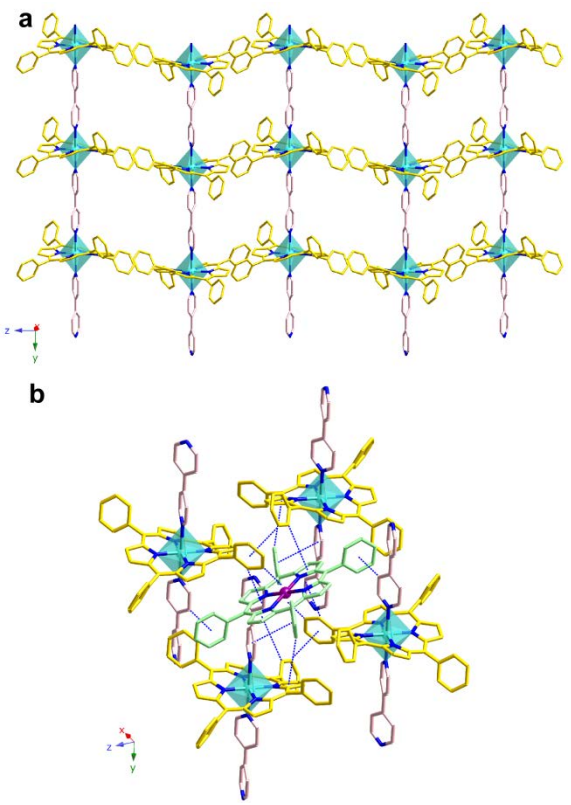


**Fig. 1** View of the structure for compound **1** where the packing of the 1D polymers is observed (a). Detail of the structure showing a single crystallization molecule of TPP connected to four 1D polymers through the π-bonding system (dashed lines) (b). Color codes: Co(1) (TPP chain) in turquoise, Co(2) (isolated TPP) in purple, N in blue, C (TPP chain) in yellow, C (isolated TPP) in green, C (bipy) in pink. H atoms have been omitted for clarity.

Additionally, isolated TPP units are located in the voids (3.4 x 3.4 Å) generated by the packing of these chains, due to an intricate system of π bonds (Fig. 1b). 78% of these isolated porphyrin units are metal-free, while the remaining 22% are metallated, in accordance with the chemical formula obtained by single crystal X-ray diffraction and elemental analysis $[CoTPP(bipy)]\cdot([CoTPP])_{0.22}\cdot(TPP)_{0.78}$. Therefore, most of the CoTPP units have lost the metal ion during the synthesis. Each isolated TPP unit is surrounded by four 1D polymers producing a dense network. As observed, there are multiple *edge-to-face* π-interactions stabilising the crystal structure. These are robust interactions (distances from 2.45 Å to 2.97 Å, and angles from 73.96º to 89.16º), that are accompanied by weaker *face-to-face* ones (centroid-to-centroid distance 4.04 Å, and angle is 10.77º). (Table S7, ESI†).

The bond distances and angles for Co(1) and Co(2) coordination spheres in compound **1** lie among typical values (Table S8, ESI†). It must be pointed out that Co(1) atom lies on a two-fold axis, and Co(2) on an inversion centre. As a result, both polyhedra are close to ideal.

Topological features for compound **1** have been analysed by means of the TOPOS software.[55] The simplification shows the connectivity due to the π-bond system (Fig. S5, ESI†). Due to the nature of these intermolecular interactions no classification of the topology is provided.

Considering the isolated molecules of porphyrin in compound **1**, it was tested in order to explore its capability as a catalyst for the oxidation of water. Unfortunately, these tests demonstrated no catalytic activity (Fig. S6, ESI†).

Compound **2** has the chemical formula $[CoTPPS_{0.5}(bipy)(H_2O)_2]\cdot 6H_2O$, and exhibits some similarities with compound **1**. In fact, compound **2** also consists of 1D polymers where CoTPPS units are axially bonded to bipy ligands. However, the extension of the 1D polymers for compound **2** consists of the link between alternating metal centres along the [001] direction. These links take place through the bipy ligands according to the bipy-CoTPPS-bipy-$Co(H_2O)_4$- fashion. From a crystallographic point of view, this is an unprecedented bimetallic chain for this type of systems (Fig. 2).

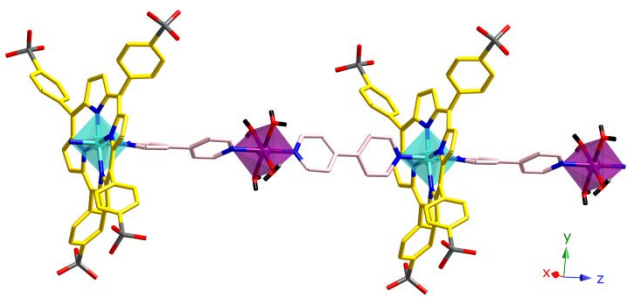

**Fig. 2** Detail of the structure for compound **2** showing the extension of the 1D polymers. Color codes: Co(1) (TPPS) in turquoise, Co(2) in purple, N in blue, C (TPPS) in yellow, C (bipy) in pink, O in red, S in grey. H atoms have been omitted for clarity.

Compound **2** exhibits a robust system of hydrogen bonds that reinforce the stability of the framework (Table S9, ESI†). This way, each chain is surrounded by another four, and multiple hydrogen bonds are formed between the coordination molecules of water and the terminal $SO_3$ groups of the TPPS molecules.

As observed in Fig. 3, the relative position of the chains give rise to cavities where crystallisation molecules of water are

located. These molecules form a disordered chain along the [001] direction, reinforcing the robustness of the hydrogen-bond system.

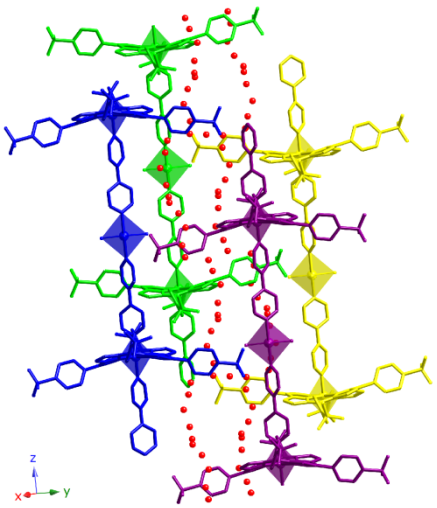

**Fig. 3** Detail of the structure showing relative position of the chains for compound **2**. Crystallisation molecules of water are shown in red. H atoms have been omitted for clarity.

As mentioned below, compound **2** exhibits a remarkable thermal stability that is related to its crystal structure. Therefore, topological features for compound **2** were analysed by means of the TOPOS software,[55] revealing a pcu α-Po primitive cubic 6/4/c1 sqc1 net.[56] As shown in Fig. 4 this consists on a two-fold interpenetrated 6-c nets framework (Point Symbol= $4^{12}.6^3$ and Vertex Symbol= 4.4.4.4.4.4.4.4.4.4.4.*.*.*).

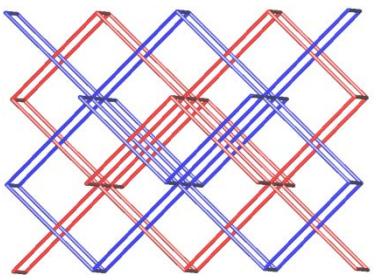

**Fig. 4** Topology of the two-fold interpenetrated net for compound **2**.

## Distortion of coordination spheres for metal centers

Distortion of coordination polyhedra as been evaluated according to Avnir[57,58] method, based on the continuous symmetry measures (CSM), by means of SHAPE program,[59] and the results can be seen on Table 2.

**Table 2** Distortion values calculated for the hexacoordinated and tetracoordinated spheres (calculated by means of SHAPE software).

| | Hexacordinate | $S(O_h)$ | $S(D_{3h})$ |
|---|---|---|---|
| Compound **1** | Co(1) | 0.68 | 17.25 |
| Compound **2** | Co(1) | 0.07 | 15.76 |
| | Co(2) | 0.02 | 16.33 |
| | **Tetracoordinate** | $S(D_{4h})$ | $S(T_d)$ |
| Compound **1** | Co(2) | 0.004 | 33.34 |

*S*= symmetry

The projection of the as-calculated values on the distortion diagram[60] can be seen in Fig. 5. As observed, for compound **1** there is a weak Jahn-Teller distortion for Co(1), in fact the axial Co(1)–N(3) distance is longer than equatorial ones, and the *cis* and *trans* N-Co(1)-N angles go from 89.79(6) to 90.21(6)º, and from 179.68(8) to 180.00(4)º, respectively. For the tetracoordinated cobalt centre, the Co(2)-N distances go from 2.032(1) to 2.055(1) Å and the *cis* and *trans* angles are close to 90 and 180º, respectively. Thus, the distortion values indicate that the coordination geometry is close to an ideal square planar sphere for Co(2). All bond distances and angles are reported in Table S10, ESI†.

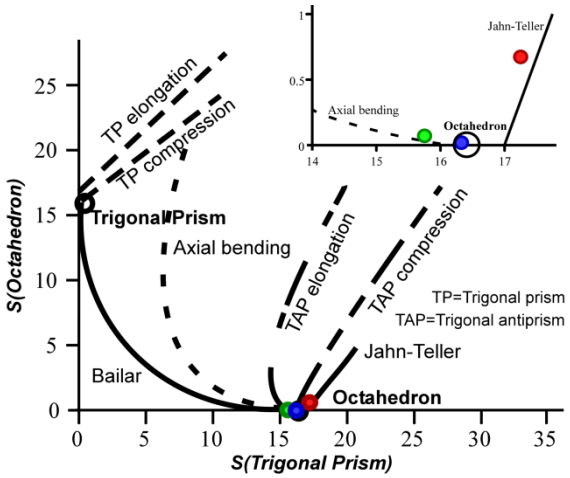


**Fig. 5** Distortion modes diagram of an octahedron. In the upper right is a zoom of the distortion for compound **1** Co(1) octahedra (red circle), and for compound **2** Co(1) (green circle) and Co(2) (blue circle) spheres.

Distortion of coordination polyhedra was also evaluated for compound **2** (Table 2), and the results indicate that, while Co(2) octahedra is nearly ideal, the Co(1) sphere exhibits weak axial bending distortion. Both metal atoms lie on a four-fold inversion, where all Co(1)–N are equal (1.963(3) Å). Obviously, the same occurs for Co(2)–O equatorial distances (2.092(3) Å). On the other hand, *cis* and *trans* angles for Co(1) go from 88.20(7) to 91.80(7)º and for 176.4(1) to 180.0º, respectively. For Co(2) octahedra these angles vary from 89.24(6) to 90.76(6)º and from 178.05(1) to 180.0º resulting in a perfect octahedra (Fig. 2). All bond distances and angles are reported in Table S11, ESI†.

## Distortion of porphyrins

Distortion of macrocycles has been also analysed for compounds **1** and **2**. There are six types of distortion defined for non-planar porphyrins: saddle (*sad*), ruffle (*ruf*), dome (*dom*), wavy(x) (*wav*(x)), wavy(y) (*wav*(y)) and propeller (*pro*).

The out-of-plane distortion of the porphyrin macrocycles was analysed by the normal-coordinate structural decomposition method developed by Shelnutt *et al.* (NSD).[61,62]

For compound **1** the results indicate a ruffle-type distortion (*ruf*, $B_{1u}$) for the coordinated porphyrin, and a slight wavy one (*wav(y)*, [$E_{g(y)}$]) for the crystallisation complex. The contribution of the ruffled porphyrin (1.4813) to the total displacements is 82.5%, while the wavy porphyrin shows a principal contribution of *wav(y)* (-0.1910) mixed with a small amount of the *wav(x)* (0.0884) deformation. The contribution of each type is 68.3% and 31.6%, respectively.

In compound **2** the principal distortion corresponds to the ruffled type (1.3203 and 67.8% of the total displacements), but the saddle-type (*sad*, $B_{2u}$) is also observed (0.6261 and 32.2%).

As shown in Fig. 6, for compounds **1** and **2**, the occurrence of ruffled-type deformation for the polymeric porphyrins, means that the *meso* carbons (non-pyrrolic carbon atoms) are alternatively above and below the porphyrin mean plane, while the pyrrole nitrogens are placed on the plane. In compound **2**, the saddle contribution is observed by the distribution of the pyrrole rings. In fact, an opposing pair of pyrrole rings tilts up, while the other pair tilts down.

The crystallisation molecule of porphyrin in compound **1** shows the two opposing pyrrole rings tilted up and down with respect to the porphyrin mean plane, indicating a wavy distortion. However, due to the small out-of-plane displacement this porphyrin is nearly planar.

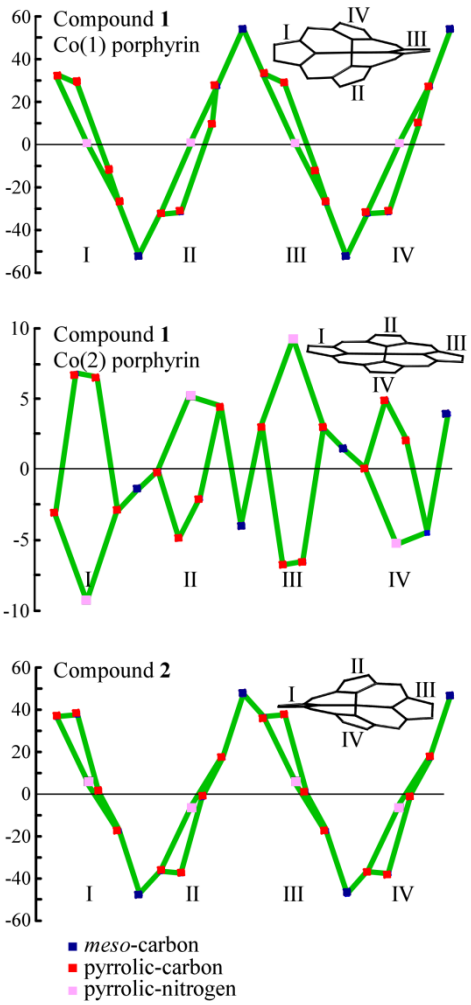


**Fig. 6** Out-of-plane displacements (in units of 0.01 Å) of the porphyrin core atoms from the mean porphyrin plane (of 24 atom). Co(1) coordinated porphyrin and Co(2) crystallization porphyrin.

There are some studies in literature exploring the relationships between the ruffle distortion and some structural parameters. However, they are referred to $Co^{III}$ compounds.

Cullen *et al.*[63] proposed the use of the *cis* and *trans* $C_\alpha$-N-N-$C_\alpha$ torsion angles as a quantitative measure of ruffling. Inspired by this work, we have analysed the *cis* and *trans* $C_\alpha$-N-N-$C_\alpha$ dihedral angles ($C_\alpha$ is a pyrrolic carbon atom bonded to a nitrogen atom) (Fig 7) for our ruffled porphyrins.

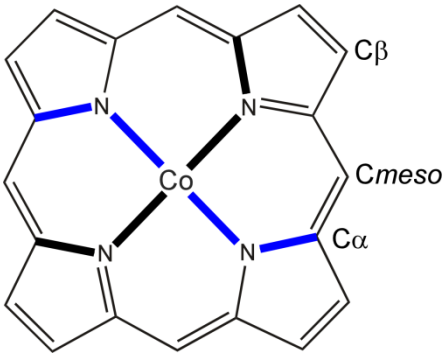


**Fig. 7** Porphyrin macrocycle and nomenclature used. *Cis* $C_\alpha$-N-N-$C_\alpha$ dihedral angle is shown in bold and *trans* $C_\alpha$-N-N-$C_\alpha$ dihedral angle in blue.

The average value for *cis* dihedral angles of **1** (31.6º(1)) is higher than for **2** (28.4º(1)). This is in accordance for the conclusions for $Co^{III}$ compounds, since the higher the *cis* dihedral angle is, the higher ruffle distortion is expected.

The average value for *trans* dihedral angles are 145.7º(1), for **1**; and 151.6º(1), for **2**. Distortion values found for compounds **1** and **2** are expected to produce values of (145º(1)) and (148.7º(1)), respectively, for $Co^{III}$ compounds.[63] As observed, the prediction for **2** is not that good, probably due to the occurrence of saddle distortion. Therefore, conclusions by Cullen *et al.* seem to be effective for $Co^{II}$ compounds.

On the other hand, Iimura *et al.*[50] found a linear relationship between the ruffled distortion and the Co-$N_p$ distances ($N_p$ are the pyrrolic nitrogen atoms) for $Co^{III}$ porphyrins.

Due to the lack of correlation studies for $Co^{II}$ compounds, we have performed a search on the Cambridge Structural Database (CSD)[64] v5.33 to find all the Co porphyrin complexes. This research indicated the existence of 221 cobalt-based metalloporphyrins, 124 of them containing $Co^{III}$. We have analysed the remaining 97 $Co^{II}$ compounds (Fig. 8).

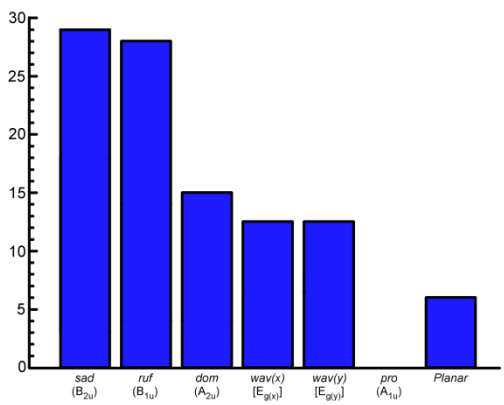


**Fig. 8** Out-of-plane distortion distribution for $Co^{II}$ porphyrins.

As observed in Fig. 8 the most typical distortion for $Co^{II}$ porphyrins are *sad* and *ruf*. As the main distortion observed for compounds **1** and **2** is the ruffle-type, we have performed a study with the 28 compounds found in literature exhibiting the same type of distortion, to establish the relationship with Co-$N_p$ distances ($N_p$ are the pyrrolic nitrogen atoms).

Fig. 9 shows a linear relationship between ruffle distortion and Co-$N_p$ distances for $Co^{II}$ compounds. As observed for $Co^{III}$ compounds, we have also found that the presence of low ruffled distortion leads to longer Co-Np distances. In particular, for compounds **1** and **2**, with distances of 1.964(1) and 1.963(3) Å, respectively, a value of 1 is expected for the distortion. Therefore, real values (1.4813 and 1.3203, respectively) lie among the typical ones.

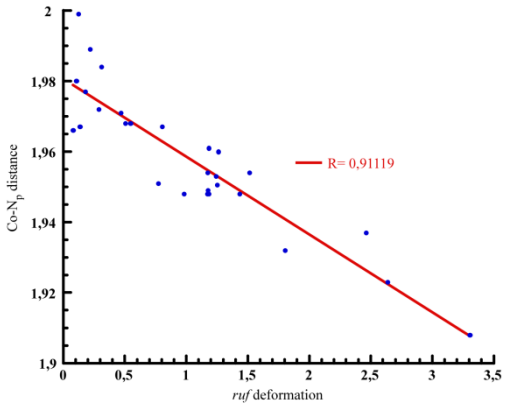


**Fig. 9** Plot of the average $Co^{II}$-$N_p$ distance *vs*. the amount of ruffled ($B_{1u}$) deformation.

### Electronic paramagnetic resonance

Electron paramagnetic resonance (EPR) measurements were performed for compounds **1** (Fig. S7, ESI†) and **2**. (Fig. S8, ESI†). The simulation of the EPR spectrum for both compounds gave us the following set of values: $g_\perp$=2.232 and $g_\parallel$=2.030 for compound **1**, and $g_1$=5.7, $g_2$=3.95 and $g_3$= 3.42 for **2**. The main signal for compound **1** is due to Co(1) atom, and it is in accordance with an octahedral low-spin $Co^{II}$ ion. For compound **2**, the signal is the sum of the contribution of both metal centres. The observed value for the sum of the three orthogonal g values ($g_s$=13.07) is in excellent agreement with the theoretical value near 13 proposed by Abragam and Pryce[65], in accordance with an octahedral high-spin $Co^{II}$.

### Thermogravimetry

The thermogravimetric decomposition curve for compound **1** shows a two-stage mass loss. The first step occurs between 230-290 ºC with 10.6 % weight loss, and the second one from 410 ºC to 500 ºC with 81 % weight loss. These values have been attributed to bipyridine (10.7 %) and to isolated and polymeric TPP units (84.3 %) (Fig. S9, ESI†). The residue has been identified by X-ray powder diffraction as $Co_3O_4$ [S.G. *Fd*-3*m*, a = 8.11 Å].[66]

Compound **2** shows a two-stage mass loss. The first of them starting at RT and finishing at about 370 ºC, is a smooth decrease of mass, and has been assigned to the removal of the crystallisation molecules of water (10 % weight loss). On the contrary, the second one (approximately 81 %) is abrupt, and corresponds to the removal of the coordination molecules of water, and both organic ligands (Fig. S10, ESI†). The calcination product was also $Co_3O_4$.

### X-ray thermodiffractometry (TDX)

The thermal behaviour of compounds **1** and **2** was also studied by X-ray thermodiffractometry (Fig. 10a). Compound **1** is thermally stable until 190 ºC. At higher temperatures, the removal of the bipy ligands provokes the formation of CoTPP[67] (Fig. S11, ESI†). This phase is stable until 370 ºC, temperature at which $Co_3O_4$ is formed.

The thermal stability of compound **2** is remarkably high. In fact, TDX analysis reveals that it is stable up to 370ºC (Fig. 10b). Above this temperature an amorphous phase is formed. The robust hydrogen bond network and the fact that the structure is two-fold interpenetrated are thought to be responsible for the high thermal stability of this compound.

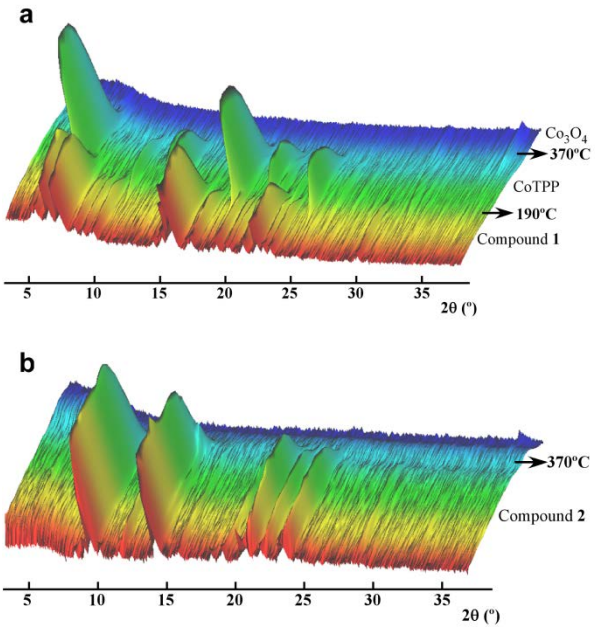


**Fig. 10** Thermodiffractogram of compound **1** (a) and for compound **2** (b).

## Conclusions

TPP and TPPS porphyrins produce 1D polymers with $Co^{II}$. Stabilisation of the network for Co-TPP compound takes place through crystallisation metalloporphyrins and molecules of porphyrin, *via* an extended π-bond system. For Co-TPPS compound an extended hydrogen bond system along with an intricate topology yields the first compound with this metalloporphyrin combination. In addition, this Co-TPPS compound exhibits an unprecedented bimetallic chain and shows a remarkably high thermal stability.

For both compounds, the distortion of the porphyrins has been observed to be ruffled-type. A crystallochemical study confirmed the existence of a correlation between the degree of ruffled distortion and Co-$N_p$ distances not only for both compounds, but also for all the $Co^{II}$ porphyrins found in the CSD.

## Acknowledgements

This work has been financially supported by the ‘‘Ministerio de Ciencia e Innovación’’ (MAT2010-15375) and the ‘‘Gobierno Vasco’’ (Basque University System Research Groups, IT-630-13) which we gratefully acknowledge. SGIker (UPV/EHU) technical support (MEC, GV/EJ, European Social Fund) is gratefully acknowledged. The authors like to thank Dr. L. Lezama

(UPV/EHU) for her help in the interpretation of EPR measurements and Prof. A. Llobet (ICIQ), Dr. X. Sala (UAB) and J. Aguiló (UAB) for the catalytic tests. A. Fidalgo-Marijuan thanks to the UPV/EHU fellowships.

## Notes and references

[a] *Departamento de Mineralogía y Petrología, Facultad de Ciencia y Tecnología, Universidad del País Vasco (UPV/EHU), Apdo. 644, 48080 Bilbao, Spain. Fax:+34 946 013 500; Tel: +34 946 015 984; E-mail: arkaitz.fidalgo@ehu.es, bego.bazan@ehu.es, karmele.urtiaga@ehu.es, maribel.arriortua@ehu.es*

[b] *Departamento de Química Inorgánica, Facultad de Farmacia, Universidad del País Vasco (UPV/EHU), Paseo de la Universidad 7, 01006 Vitoria-Gasteiz, Spain. Fax: +34 945 013 014; Tel: +34 945 013 080; E-mail: gotzone.barandika@ehu.es*

† Electronic Supplementary Information (ESI) available: Crystallographic data, IR, TGA, EPR, PXRD. CCDC 890986 and 890987. See DOI: 10.1039/b000000x/

1. J. R. Long and O. M. Yaghi, *Chem. Soc. Rev.*, 2009, **38**, 1213.
2. O. K. Farha and J. T. Hupp, *Acc. Chem. Res.*, 2010, **43**, 1166.
3. K. K. Tanabe and S. M. Cohen, *Chem. Soc. Rev.*, 2011, **40**, 498.
4. A. Fidalgo-Marijuan, G. Barandika, B. Bazan, M. K. Urtiaga and M. I. Arriortua, *Polyhedron*, 2011, **30**, 2711.
5. M. Eddaoudi, J. Kim, N. Rosi, D. Vodak, J. Wachter, M. O'Keeffe and O. M. Yaghi, *Science*, 2002, **295**, 469.
6. L. J. Murray, M. Dinca and J. R. Long, *Chem. Soc. Rev.*, 2009, **38**, 1294.
7. J.-R. Li, R. J. Kuppler and H.-C. Zhou, *Chem. Soc. Rev.*, 2009, **38**, 1477.
8. S.-C. Xiang, Z. Zhang, C.-G. Zhao, K. Hong, X. Zhao, D.-R. Ding, M.-H. Xie, C.-D. Wu, C. Das Madhab, R. Gill, K. M. Thomas and B. Chen, *Nat Commun*, 2011, **2**, 204.
9. M. D. Allendorf, R. J. T. Houk, L. Andruszkiewicz, A. A. Talin, J. Pikarsky, A. Choudhury, K. A. Gall and P. J. Hesketh, *J. Am. Chem. Soc.*, 2008, **130**, 14404.
10. A. Lan, K. Li, H. Wu, D. H. Olson, T. J. Emge, W. Ki, M. Hong and J. Li, *Angew. Chem., Int. Ed.*, 2009, **48**, 2334.
11. Z. Xie, L. Ma, K. E. de Krafft, A. Jin and W. Lin, *J. Am. Chem. Soc.*, 2010, **132**, 922.
12. G. Lu and J. T. Hupp, *J. Am. Chem. Soc.*, 2010, **132**, 7832.
13. O. R. Evans and W. Lin, *Acc. Chem. Res.*, 2002, **35**, 511.
14. K. E. deKrafft, Z. Xie, G. Cao, S. Tran, L. Ma, O. Z. Zhou and W. Lin, *Angew. Chem., Int. Ed.*, 2009, **48**, 9901.
15. J. Della Rocca and W. Lin, *Eur. J. Inorg. Chem.*, 2010, 3725.
16. D. Liu, R. C. Huxford and W. Lin, *Angew. Chem., Int. Ed.*, 2011, **50**, 3696.
17. P. Horcajada, T. Chalati, C. Serre, B. Gillet, C. Sebrie, T. Baati, J. F. Eubank, D. Heurtaux, P. Clayette, C. Kreuz, J.-S. Chang, Y. K. Hwang, V. Marsaud, P.-N. Bories, L. Cynober, S. Gil, G. Ferey, P. Couvreur and R. Gref, *Nat. Mater.*, 2010, **9**, 172.
18. W. Lin, J. W. Rieter and K. M. L. Taylor, *Angew. Chem., Int. Ed.*, 2009, **48**, 650.
19. W. J. Rieter, K. M. Pott, K. M. L. Taylor and W. Lin, *J. Am. Chem. Soc.*, 2008, **130**, 11584.
20. L. Ma, C. Abney and W. Lin, *Chem. Soc. Rev.*, 2009, **38**, 1248.
21. L. Ma, J. M. Falkowski, C. Abney and W. Lin, *Nat. Chem.*, 2010, **2**, 838.
22. F.-J. Song, C. Wang, J. M. Falkowski, L.-Q. Ma and W.-B. Lin, *J. Am. Chem. Soc.*, 2010, **132**, 15390.
23. M. Banerjee, S. Das, M. Yoon, H. J. Choi, M. H. Hyun, S. M. Park, G. Seo and K. Kim, *J. Am. Chem. Soc.*, 2009, **131**, 7524.
24. J. P. Collman, R. Boulatov, C. J. Sunderland and L. Fu, *Chem. Rev.*, 2004, **104**, 561.
25. R. A. Sheldon, in *Metalloporphyrins in Catalytic Oxidations*, ed. R. A. Sheldon, Marcel Dekker, Inc., New York, 1994.
26. X.-L. Yang, M.-H. Xie, C. Zou, Y. He, B. Chen, M. O'Keeffe and C.-D. Wu, *J. Am. Chem. Soc.*, 2012, **134**, 10638.
27. K. S. Suslick, P. Bhyrappa, J. H. Chou, M. E. Kosal, S. Nakagaki, D. W. Smithenry and S. R. Wilson, *Acc. Chem. Res.*, 2005, **38**, 283.
28. I. Beletskaya, V. S. Tyurin, A. Y. Tsivadze, R. Guilard and C. Stern, *Chem. Rev.*, 2009, **109**, 1659.
29. C. M. Drain, A. Varotto and I. Radivojevic, *Chem. Rev.*, 2009, **109**, 1630.
30. I. Goldberg, *CrystEngComm*, 2008, **10**, 637.
31. L. D. DeVries and W. Choe, *J. Chem. Crystallogr.*, 2009, **39**, 229.
32. C. Zou and C.-D. Wu, *Dalton Trans.*, 2012, **41**, 3879.
33. R. K. Kumar, S. Balasubramanian and I. Goldberg, *Chem. Commun.*, 1998, 1435.
34. A. Calderon-Casado, G. Barandika, B. Bazan, M. K. Urtiaga, O. Vallcorba, J. Rius, C. Miravittles and M. I. Arriortua, *CrystEngComm*, 2011, **13**, 6831.
35. M. G. Barandika, M. L. Hernandez-Pino, M. K. Urtiaga, R. Cortes, L. Lezama, M. I. Arriortua and T. Rojo, *J. Chem. Soc., Dalton Trans.*, 2000, 1469.
36. M. G. Barandika, R. Cortes, Z. Serna, L. Lezama, T. Rojo, M. K. Urtiaga and M. I. Arriortua, *Chem. Commun.*, 2001, 45.
37. N. de la Pinta, S. Martin, M. K. Urtiaga, M. G. Barandika, M. I. Arriortua, L. Lezama, G. Madariaga and R. Cortes, *Inorg. Chem.*, 2010, **49**, 10445.
38. M. L. Hernandez, M. K. Urtiaga, M. G. Barandika, R. Cortes, L. Lezama, N. de la Pinta, M. I. Arriortua and T. Rojo, *J. Chem. Soc., Dalton Trans.*, 2001, 3010.
39. Z. F. Serna, L. Lezama, M. K. Urtiaga, M. I. Arriortua, M. G. Barandika, R. Cortes and T. Rojo, *Angew. Chem., Int. Ed.*, 2000, **39**, 344.
40. H. Kanemitsu, R. Harada and S. Ogo, *Chem Commun*, 2010, **46**, 3083.
41. W.-T. Chen, Y. Yamada, G.-N. Liu, A. Kubota, T. Ichikawa, Y. Kojima, G.-C. Guo and S. Fukuzumi, *Dalton Trans.*, 2011, **40**, 12826.
42. W.-T. Chen, Z.-G. Luo, J.-H. Liu, H.-L. Chen and H.-M. Kuang, *J. Chem. Res.*, 2011, **35**, 571.
43. R. K. Kumar, Y. Diskin-Posner and I. Goldberg, *J. Inclusion Phenom. Macrocyclic Chem.*, 2000, **37**, 219.
44. A. L. Litvinov, D. V. Konarev, A. Y. Kovalevsky, I. S. Neretin, P. Coppens and R. N. Lyubovskaya, *Cryst. Growth Des.*, 2005, **5**, 1807.
45. J. A. Shelnutt, in *The Porphyrin Handbook*, Academic Press, eds. K. M. Kadish, K. M. Smith, R. Guilard, New York, Academic Press, vol. 7, 2000.
46. N. Karakostas, D. Schaming, S. Sorgues, S. Lobstein, J. P. Gisselbrecht, A. Giraudeau, I. Lampre and L. Ruhlmann, *J. Photochem. Photobiol., A*, 2010, **213**, 52.

47. F. Nifiatis, W. Su, J. E. Haley, J. E. Slagle and T. M. Cooper, *J. Phys. Chem. A*, 2011, **115**, 13764.
48. P. Bhyrappa and K. Karunanithi, *Inorg. Chim. Acta*, 2011, **372**, 417.
49. Z. Zhou, C. Cao, Q. Liu and R. Jiang, *Org. Lett.*, 2010, **12**, 1780.
50. Y. Iimura, T. Sakurai and K. Yamamoto, *Bull. Chem. Soc. Jpn.*, 1988, **61**, 821.
51. W. Yinghua, *J. Appl. Crystallogr.*, 1987, **20**, 258.
52. A. Altomare, G. Cascarano, C. Giacovazzo and A. Guagliardi, *J. Appl. Crystallogr.*, 1993, **26**, 343.
53. G. M. Sheldrick, *Acta Crystallogr., Sect. A Found. Crystallogr.*, 2008, **A64**, 112.
54. L. Palatinus and G. Chapuis, *J. Appl. Crystallogr.*, 2007, **40**, 786.
55. V. A. Blatov, *IUCr CompComm Newsl.*, 2006, 4 http://www.topos.ssu.samara.ru.
56. H. Chung, P. M. Barron, R. W. Novotny, H.-T. Son, C. Hu and W. Choe, *Cryst. Growth Des.*, 2009, **9**, 3327.
57. H. Zabrodsky, S. Peleg and D. Avnir, *J. Am. Chem. Soc.*, 1992, **114**, 7843.
58. M. Pinsky and D. Avnir, *Inorg. Chem.*, 1998, **37**, 5575.
59. M. Llunel, D. Casanova, J. Cirera, J. M. Bofill, P. Alemany, S. Álvarez, M. Pinsky and D. Yatunir, *SHAPE v1.1a, "Program for Continuous Shape Measure Calculations of Polyhedral Xn and MLn Fragments"* edn., 2003.
60. S. Álvarez, P. Alemany, D. Casanova, J. Cirera, M. Llunell and D. Avnir, *Coord. Chem. Rev.*, 2005, **249**, 1693.
61. W. Jentzen, X.-Z. Song and J. A. Shelnutt, *J. Phys. Chem. B*, 1997, **101**, 1684.
62. W. Jentzen, J.-G. Ma and J. A. Shelnutt, *Biophys. J.*, 1998, **74**, 753.
63. D. L. Cullen, L. V. Desai, J. A. Shelnutt and M. Zimmer, *Struct. Chem.*, 2001, **12**, 127.
64. F. H. Allen, *Acta Crystallogr., Sect. B Struct. Sci.*, 2002, **B58**, 380.
65. A. Abragam and M. H. L. Pryce, *Proc. R. Soc. London, Ser. A*, 1951, **206**, 173.
66. J. D. Hanawalt, H. W. Rinn and L. K. Frevel, *Ind. Eng. Chem., Anal. Ed.*, 1938, **10**, 457.
67. B. F. O. Nascimento, M. Pineiro, A. M. d. A. Rocha Gonsalves, M. R. Silva, A. M. Beja and J. A. Paixao, *J. Porphyrins Phthalocyanines*, 2007, **11**, 77.